Inorganic Chemistry

pubs.acs.org/IC Article

Strategy for Traceless Codrug Delivery with Platinum(IV) Prodrug Complexes Using Self-Immolative Linkers

Violet Eng Yee Lee, Zhi Chiaw Lim, Suet Li Chew, and Wee Han Ang*

Cite This: *Inorg. Chem.* 2021, 60, 1823−1831 Read Online

ACCESS | Metrics & More | Article Recommendations | Supporting Information

ABSTRACT: A common challenge in Pt(IV) prodrug design is the limited repertoire of linkers available to connect the Pt(IV) scaffold with the bioactive payload. The commonly employed linkers are either too stable, leading to a linker artifact on the payload upon release, or too unstable, leading to premature release. In this study, we report the synthesis of a new class of Pt(IV) prodrugs using masked self-immolative 4-aminobenzyl linkers for controlled and traceless codrug delivery. Upon reduction of self-immolative Pt(IV) prodrugs, the detached axial ligands undergo decarboxylation and 1,6-elimination for payload release. Introduction of self-immolative linkers conferred good aqueous stability to the Pt(IV) codrug complex. Investigation revealed that efficient 1,6-elimination could be attributed to stabilization of the *p*-aza-quinone-methide intermediate. In particular, the self-immolative Pt(IV) prodrugs with cinnamate and coumarin derivatives were more potent than the coadministration of cisplatin with an unconjugated cinnamate or coumarin payload in vitro.

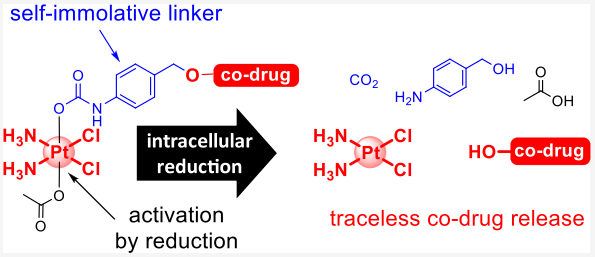

INTRODUCTION

Food and Drug Administration (FDA)-approved cisplatin (cDDP) is a leading Pt(II) anticancer drug administered clinically to treat various malignancies such as ovarian, testicular, head, and neck cancers.[1] However, the efficacy of cDDP is diminished due to its dose-limiting systematic toxicity and chemoresistance.[2] Thus, a combination therapy involving cDDP with one or more anticancer drugs is commonly administered as each drug acts via different molecular mechanisms and can deter drug resistance.[3,4] Yet, the promising results of combination therapy on 2D tissue cultures in vitro may not be replicated in vivo in complex organisms as each chemotherapeutic drug has different pharmacological properties with different biodistribution profiles that diminish the effectiveness of the synergistic or complementary combination therapy.[5,6] Pt(IV) prodrug is an useful strategy that serves as a delivery vessel to simultaneously deliver ratiometric amounts of cDDP and combination drugs upon activation by biological reducing agents.[7] Furthermore, since the Pt(IV) prodrug is kinetically stable, it is resistant to unwanted reactions with plasma proteins and prevents side-effects associated with cDDP and combination drugs.[8]

The direct conjugation to the axial ligand position of a Pt(IV) scaffold requires specific functionalities often absent in chemotherapeutic drugs such as paclitaxel,[9] doxorubicin,[10,11] docetaxel,[12] and gemcitabine[13] used in combination with cDDP.[14,15] Often, covalent ether, amide, or ester linkers are employed to conjugate bioactive ligands, for example, chalcone,[16] 7-hydroxycoumarin,[17] combretastatin-A4,[18] and estrogen,[19] to Pt(IV) scaffolds. Covalent linkages including ether, amide, and oxime are highly stable and not readily released from the codrug payload.[11,20,21] On the other hand, ester linkers are readily hydrolyzed or cleaved by esterases, leading to unintended and premature release during circulation.[22] Such conventional linkers limit the implementation of controlled simultaneous dual-drug delivery into cancer cells for a maximum therapeutic effect. Recently, carbamate and carbonate linkers have been reported as efficient linkers that release conjugated drugs upon reduction of Pt(IV) prodrugs.[22−24] We present a new strategy for cDDP-based Pt(IV) prodrugs that incorporate the self-immolative 4-aminobenzyl alcohol (4ABA) linker that could undergo a *p*-aza-quinone-methide 1,6-elimination self-immolative reaction for a controlled dual-drug delivery.[25] Upon intracellular reduction, these Pt(IV) prodrug complexes would release axial ligands that could undergo decarboxylation and sequentially trigger self-immolation to restore the codrug.

To that end, we prepared a series of functionalized Pt(IV) prodrug complexes with a therapeutic payload tethered to self-immolative linkers as a proof of concept and investigated their release kinetics (Figure 1). Methyl *trans*-2-hydroxycinnamate (MeHC) and 7-hydroxy-3-methylcoumarin (7-HMC) were

Received: November 5, 2020
Published: January 19, 2021

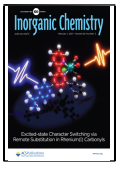

https://dx.doi.org/10.1021/acs.inorgchem.0c03299
Inorg. Chem. 2021, 60, 1823−1831

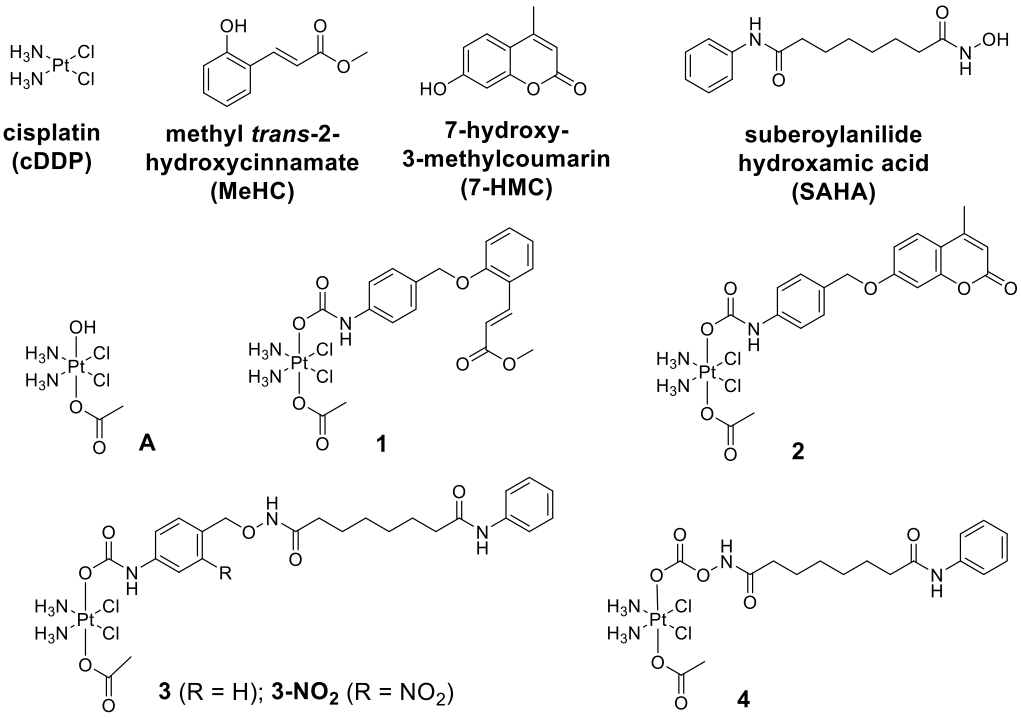

Figure 1. Molecular structures of cDDP, model codrug payloads, Pt(IV) precursor **A**, and functionalized Pt(IV) complexes **1**−**4**.

chosen as model codrugs as they are privileged scaffolds of natural products with known therapeutic effects against cancer.[17,26] Suberoylanilide hydroxamic acid (SAHA) is an FDA-approved histone deacetylase inhibitor (HDACi)[27,28] and the combination therapy of SAHA and cDDP has been reported to produce a synergistic effect in inducing cancer cell death.[29−31] Because the self-immolative linkers could spontaneously decompose, we developed a synthesis approach that initially masked the trigger group before carrying out functional group transformation for direct coupling with the Pt(IV) scaffold. We investigated their self-immolation kinetics and demonstrated that the unmodified payload could be released upon reduction at the Pt(IV) center. We also investigated the efficacy of these novel prodrug complexes against established HeLa, A2780, and A2780cis cell lines.

EXPERIMENTAL SECTION

Materials and Methods. All experiments were carried out with no exclusion of moisture and air. All chemicals and solvents were handled without further treatment. All chemicals and solvents were of analytical or high-performance liquid chromatography (HPLC) grade and were purchased commercially. ^{1}H, ^{195}Pt, and ^{13}C nuclear magnetic resonance (NMR) spectra were recorded using a Bruker AMX 400 spectrometer and a Bruker AMX 500 spectrometer. ^{195}Pt NMR spectra were externally referenced using K_2PtCl_4. Mass spectra were measured with a Finnigan MAT LCQ (ESI) spectrometer. [Pt] was determined by inductively-coupled plasma−optical emission spectroscopy (ICP−OES) by CMMAC, NUS. The HPLC system consisted of a vacuum degasser (Agilent model G1322A), a quaternary pump (Agilent model G1311A), an autosampler (Agilent model G1329A), a thermostated column compartment (Agilent model G1316A), and a diode array detector (Agilent model G1315A). Reversed-phase−HPLC (RP-HPLC) purification was performed using an Agilent 1200 DAD with a Shim-pack VP-C18 column (5 μm, 100 Å, 250 mm × 4.6 mm) at a flow rate of 1.5 mL/min. The eluents used were H_2O (A) and MeCN (B). The gradient elution was 20% B to 70% B from 0 to 50 min, and the column was flushed at 90% B for washing for 10 min and re-equilibrated to 20% B for 10 min. The stabilities, purities, and reactions of Pt(IV) compounds were determined using an Agilent Eclipse Plus C18 (5 μM, 4.60 × 12.5 mm i.d) column at 254 and 280 nm wavelengths, and the flow rate used was 1.0 mL/min. The eluents used were H_2O (A) and MeCN (B). The gradient elution was 20% A to 90% B from 0 to 20 min. Fluorescence measurements were carried out with a BioTek Synergy H1 hybrid multimode microplate reader. cDDP[32] and **A**[33] were synthesized according to the procedures reported in the literature.

Synthesis of MeHC. 2-Coumaric acid (328 mg, 2.00 mmol) was suspended in MeOH (10 mL) and concentrated H_2SO_4 (0.37 mL) was added. The reaction mixture was stirred at room temperature (r.t.) for 24 h and then concentrated in vacuo. The residue was dissolved in H_2O (8 mL) and extracted with diethyl ether. Organic layers were combined, washed with H_2O, saturated Na_2CO_3, and brine, and dried over Na_2SO_4. The solution was filtered and dried in vacuo to give the desired product as a white precipitate. Yield: 278 mg (78%). ^{1}H NMR (400 MHz, DMSO-d_6) δ 10.24 (s, 1H, OH), 7.88 (d, J = 16.2 Hz, 1H, =CHAr), 7.59 (d, J = 7.8 Hz, 1H, Ar−H), 7.24 (m, 1H, Ar−H), 6.91 (d, J = 8.1 Hz, 1H, Ar−H), 6.86−6.79 (m, 1H, Ar−H), 6.61 (d, J = 16.2 Hz, 1H, =CHCO$_2$), 3.71 (s, 3H, CH$_3$). ^{13}C NMR (101 MHz, DMSO-d_6) δ 167.15, 156.78, 140.14, 131.72, 128.83, 120.67, 119.39, 116.84, 116.16, 51.29. ESI−MS (−ve mode): m/z = 177.1 [M−H]$^-$. RP-HPLC purity: 99.4% (254 nm) and 99.0% (280 nm); t_r = 15.3 min.

Synthesis of SAHA.[34] Yield: 73%. ^{1}H NMR (300 MHz, DMSO) δ 10.32 (s, 1H, CONHOH), 9.84 (s, 1H, CONH), 8.65 (s, 1H, NHOH), 7.58 (d, J = 7.6 Hz, 2H, Ar−H), 7.27 (t, J = 7.9 Hz, 2H, Ar−H), 7.01 (t, J = 7.4 Hz, 1H, Ar−H), 2.28 (t, J = 7.4 Hz, 2H, CH$_2$CONHOH), 1.93 (t, J = 7.3 Hz, 2H, CH$_2$CONHAr), 1.64−1.41 (m, 4H, CH$_2$CH$_2$), 1.27 (d, J = 3.5 Hz, 4H, CH$_2$CH$_2$). ^{13}C NMR (126 MHz, DMSO) δ 171.16, 169.05, 139.31, 128.56, 122.84, 119.00, 36.32, 32.20, 28.36, 24.97. ESI−MS (−ve mode): m/z = 264.3 [M−H]$^-$. RP-HPLC purity: 95.6% (254 nm) and 96.1% (280 nm); t_r = 8.36 min.

General Procedure for Intermediate L1 and L2. MeHC or 7-HMC (1 equiv) was dissolved in MeOH (10 mL). 4-Bromomethylbenzoic acid (1.5 equiv) and K_2CO_3 (2 equiv) were added to the reaction mixture and stirred at r.t. for 18 h, and thin layer chromatography was used to monitor the reaction progress. The

https://dx.doi.org/10.1021/acs.inorgchem.0c03299
Inorg. Chem. 2021, 60, 1823−1831

reaction mixture was concentrated in vacuo and the residue was redissolved in H_2O and acidified to pH 1 with 1 M HCl. The residue was collected, washed with H_2O and diethyl ether, and dried. The pure product was purified with flash column chromatography with an eluent system of EA/*n*-hexane (2:3 v/v).

L1. Yield: 43%. ^{1}H NMR (400 MHz, DMSO-d_6) δ 12.97 (s, 1H, COOH), 8.01−7.90 (m, 3H, =CHAr and Ar−H), 7.74 (dd, J = 7.7, 1.7 Hz, 1H, Ar−H), 7.57 (d, J = 8.4 Hz, 2H, Ar−H), 7.45−7.35 (m, 1H, Ar−H), 7.15 (d, J = 7.9 Hz, 1H, Ar−H), 7.01 (t, J = 7.5 Hz, 1H, Ar−H), 6.64 (d, J = 16.2 Hz, 1H, =$CHCO_2$), 5.32 (s, 2H, CH_2), 3.70 (s, 3H, CH_3). ^{13}C NMR (101 MHz, DMSO-d_6) δ 167.03, 166.92, 156.68, 141.74, 139.16, 131.98, 130.36, 129.58, 128.84, 127.42, 122.63, 121.18, 118.16, 113.17, 69.18, 51.43. ESI−MS (−ve mode): m/z = 311.0 $[M-H]^-$.

L2. Yield: 48%. ^{1}H NMR (400 MHz, DMSO-d_6) δ 12.99 (s, 1H, COOH), 8.00−7.94 (m, 2H, Ar−H), 7.71 (d, J = 8.7 Hz, 1H, Ar−H), 7.58 (d, J = 8.3 Hz, 2H, Ar−H), 7.11−7.03 (m, 2H, Ar−H), 6.22 (d, J = 1.3 Hz, 1H, =CH), 5.33 (s, 2H, CH_2), 2.40 (s, 3H, CH_3). ^{13}C NMR (126 MHz, DMSO-d_6) δ 167.06, 161.13, 160.09, 154.66, 153.39, 141.27, 130.52, 129.53, 127.52, 126.59, 113.45, 112.69, 111.35, 101.76, 69.20, 18.14. ESI−MS (−ve mode): m/z = 309.1 $[M-H]^-$.

General Procedure for Intermediate L3 and L3−NO_2. SAHA (1 equiv) was dissolved in MeOH (10 mL). 4-Bromomethylbenzoic acid or 4-bromomethyl-3-nitrobenzoic acid (1 equiv) was added to the reaction mixture followed by addition of 40% w/v NaOH dropwise. The reaction mixture was stirred at r.t. for 18 h and then concentrated in vacuo. The remaining residue was dissolved in H_2O (6 mL) and acidified with 1 M HCl to pH 1. The white precipitate was collected, dried, and used without further purification.

L3. Yield: 79%. ^{1}H NMR (500 MHz, DMSO-d_6) δ 12.93 (brs, 1H, COOH), 11.00 (s, 1H, CONHO), 9.84 (s, 1H, CONH), 7.98−7.94 (m, 2H, Ar−H), 7.62−7.57 (m, 2H, Ar−H), 7.54−7.49 (m, 2H, Ar−H), 7.32−7.24 (m, 2H, Ar−H), 7.02 (tt, J = 7.3, 1.2 Hz, 1H, Ar−H), 4.86 (s, 2H, CH_2), 2.29 (t, J = 7.5 Hz, 2H, CH_2CONHOH), 1.96 (t, J = 7.4 Hz, 2H, CH_2CONHAr), 1.54 (t, 7.0 Hz, 4H, CH_2CH_2), 1.28 (ddt, J = 12.8, 9.5, 4.7 Hz, 4H, CH_2CH_2). ^{13}C NMR (126 MHz, DMSO-d_6) δ 171.20, 169.46, 167.19, 140.89, 139.35, 129.26, 128.62, 128.43, 122.89, 119.02, 76.12, 36.35, 32.17, 28.38, 28.28, 24.98, 24.81. ESI−MS (−ve mode): m/z = 397.1 $[M-H]^-$.

L3−NO_2. Yield: 83%. ^{1}H NMR (400 MHz, DMSO-d_6) δ 13.75 (s, 1H, COOH), 11.13 (s, 1H, CONHO), 9.83 (s, 1H, CONH), 8.50 (d, J = 1.7 Hz, 1H, Ar−H), 8.28 (dd, J = 8.0, 1.7 Hz, 1H, Ar−H), 7.93 (d, J = 8.0 Hz, 1H, Ar−H), 7.58 (d, J = 7.6 Hz, 2H, Ar−H), 7.33−7.21 (m, 2H, Ar−H), 7.01 (t, J = 7.4 Hz, 1H, Ar−H), 5.22 (s, 2H, CH_2), 2.28 (t, J = 7.4 Hz, 2H, CH_2CONHOH), 1.94 (t, J = 7.3 Hz, 2H, CH_2CONHAr), 1.51 (m, 4H, CH_2CH_2), 1.34−1.16 (m, 4H, CH_2CH_2). ^{13}C NMR (126 MHz, DMSO-d_6) δ 171.20, 169.85, 165.40, 139.34, 136.44, 133.84, 131.74, 130.50, 128.63, 125.19, 122.91, 119.03, 73.13, 36.35, 32.08, 28.37, 28.26, 24.98, 24.71. ESI−MS (−ve mode): m/z = 442.1 $[M-H]^-$.

General Procedure for 1−3 and 3−NO_2. A self-immolative linker-modified drug (2.4 equiv) was dissolved in DMSO (1 mL). NEt_3 (2.4 equiv) was added to the solution and stirred for 5 min. DPPA (2.4 equiv) was then added and stirred at r.t. for 30 min followed by stirring for 3 h at 70 °C. After that, **A** (1 equiv) was added to the reaction mixture and stirred at 50 °C for 24 h. After completion of the reaction, the solution was filtered and dried. A pure Pt(IV) complex was obtained via purification by RP-HPLC.

1: Yield (est.): 20%. ^{1}H NMR (500 MHz, DMSO-d_6) δ 9.15 (s, 2H, CONH), 7.87 (d, J = 16.2 Hz, 1H, =CHAr), 7.75−7.66 (m, 1H, Ar−H), 7.49 (d, J = 8.4 Hz, 2H, Ar−H), 7.40 (t, J = 7.6 Hz, 1H, Ar−H), 7.28 (d, J = 8.4 Hz, 2H, Ar−H), 7.18 (d, J = 8.5 Hz, 1H, Ar−H), 6.98 (t, J = 7.5 Hz, 1H, Ar−H), 6.61 (d, J = 16.2 Hz, 7H, NH_3 and =$CHCO_2$), 5.09 (s, 2H, CH_2), 3.69 (s, 3H, CH_3), 1.93 (s, 3H, CO_2CH_3). ^{13}C NMR (126 MHz, DMSO) δ 167.02, 157.19, 157.12, 140.74, 139.48, 131.99, 128.90, 128.82, 128.34, 122.54, 121.79, 120.89, 119.91, 117.97, 113.27, 69.90, 51.44, 22.85. ^{195}Pt {^{1}H} NMR (DMSO-d_6, 108 MHz): 1169.7 ppm. ESI−MS (−ve mode): m/z = 683.8 $[M-H]^-$. RP-HPLC purity: 98.3% (254 nm) and 97.7% (280 nm); t_r = 18.6 min.

2: Yield (est.): 46%. ^{1}H NMR (500 MHz, DMSO-d_6) δ 9.15 (s, 1H, CONH), 7.68 (dd, J = 8.9, 3.2 Hz, 1H, Ar−H), 7.48 (dd, J = 8.9, 3.1 Hz, 2H, Ar−H), 7.28 (dd, J = 8.8, 3.0 Hz, 2H, Ar−H), 7.07−7.03 (m, 1H, Ar−H), 7.01 (dd, J = 8.5, 3.0 Hz, 1H, Ar−H), 6.65 (brs, 6H, NH_3), 6.20 (d, J = 2.2 Hz, 1H, =$CHCO_2$), 5.10 (s, 2H, CH_2), 2.39 (s, 3H, CH_3), 1.93 (s, 3H, CO_2CH_3). ^{13}C NMR (126 MHz, DMSO-d_6) δ 166.99, 161.48, 160.56, 160.16, 154.68, 153.45, 140.63, 130.42, 129.70, 128.36, 126.46, 113.16, 112.78, 111.15, 101.65, 69.96, 53.06, 18.14. ^{195}Pt {^{1}H} NMR (DMSO-d_6, 108 MHz): 1171.2 ppm. ESI−MS (−ve mode): m/z = 681.8 $[M-H]^-$. RP-HPLC purity: 98.3% (254 nm) and 95.9% (280 nm); t_r = 15.1 min.

3: Yield (est.): 14%. ^{1}H NMR (500 MHz, DMSO-d_6) δ 10.87 (s, 1H, CONHO), 9.84 (s, 1H, CONHAr), 9.14 (s, 1H, CO_2NH), 7.57 (d, J = 7.7 Hz, 2H, Ar−H), 7.45 (d, J = 8.5 Hz, 2H, Ar−H), 7.27 (t, J = 7.9 Hz, 2H, Ar−H), 7.20−7.17 (m, 2H, Ar−H), 7.11 (d, J = 8.1 Hz, 1H, Ar−H), 7.01 (t, J = 7.3 Hz, 1H, Ar−H), 6.64 (brs, 6H, NH_3), 4.65 (s, 2H, CH_2), 2.28 (t, J = 7.5 Hz, 2H, CH_2CONHOH), 1.93−1.61 (m, 3H, CO_2CH_3 and CH_2CONHAr), 1.50−1.46 (m, 4H, CH_2CH_2), 1.31−1.24 (m, 4H, CH_2CH_2). ^{13}C NMR (126 MHz, DMSO-d_6) δ 178.39, 171.28, 169.29, 160.58, 140.90, 139.35, 129.34, 128.66, 128.30, 122.96, 122.95, 119.06, 76.72, 36.38, 32.26, 28.41, 28.34, 25.02, 24.88, 22.85. ^{195}Pt {^{1}H} NMR (DMSO-d_6, 108 MHz): 1168.3 ppm. ESI−MS (−ve mode): m/z = 769.9 $[M-H]^-$. RP-HPLC purity: 95.2% (254 nm) and 95.3% (280 nm); t_r = 12.5 min.

3−NO_2. Yield (est.): 12%. ^{1}H NMR (400 MHz, DMSO-d_6) δ 10.96 (s, 1H, CONHO), 9.82 (s, 1H, CONHAr), 9.70 (s, 1H, CO_2NH), 8.31 (s, 1H, Ar−H), 7.66 (dd, J = 8.5, 2.2 Hz, 1H, Ar−H), 7.61−7.54 (m, 2H, Ar−H), 7.51 (d, J = 8.5 Hz, 1H, Ar−H), 7.32−7.23 (m, 2H, Ar−H), 7.04−6.97 (m, 1H, Ar−H), 6.63 (s, 6H, NH_3), 5.00 (s, 2H, CH_2), 2.28 (t, J = 7.4 Hz, 2H, CH_2CONHOH), 1.93 (m, 5H, CO_2CH_3 and CH_2CONHAr), 1.51 (m, 4H, CH_2CH_2), 1.25 (m, 4H, CH_2CH_2). ^{13}C NMR (126 MHz, DMSO-d_6) δ 178.35, 171.23, 169.60, 159.94, 148.22, 139.35, 131.06, 129.17, 128.74, 128.62, 126.50, 122.90, 119.03, 72.93, 36.36, 32.09, 28.37, 28.29, 24.98, 24.74, 22.81. ^{195}Pt {^{1}H} NMR, (DMSO-d_6, 108 MHz): 1168.6 ppm. ESI−MS (−ve mode): m/z = 815.1 $[M-H]^-$. RP-HPLC purity: 97.5% (254 nm) and 97.6% (280 nm); t_r = 14.0 min.

Synthesis of 4. To a solution of SAHA (70.3 mg, 0.266 mmol) in DMF (5 mL) at 0 °C, CDI was added. The reaction mixture was stirred at 0 °C for 2 h. **A** (40 mg, 0.106 mmol) was then added followed by stirring at r.t. for 24 h. After this, the solution was filtered and freeze-dried. Pure **1** was obtained via purification by RP-HPLC as a white solid. Yield (est.): 32%. ^{1}H NMR (500 MHz, DMSO-d_6) δ 11.45 (s, 1H, CONHO), 9.86 (s, 1H, CONHAr), 7.59 (d, J = 8.0 Hz, 3H, Ar−H), 7.28 (t, J = 7.9 Hz, 2H, Ar−H), 7.02 (t, J = 7.3 Hz, 1H, Ar−H), 6.56 (s, 6H, NH_3), 2.29 (td, J = 7.4, 1.4 Hz, 2H, CH_2CONHOH), 2.05 (t, J = 7.3 Hz, 2H, CH_2CONHAr), 1.94 (s, 3H, CH_3), 1.60−1.49 (m, 4H, CH_2CH_2), 1.32−1.26 (m, 4H, CH_2CH_2). ^{195}Pt {^{1}H} NMR (DMSO-d_6, 108 MHz): 1170.2 ppm. ESI−MS (−ve mode): m/z = 664.8 $[M-H]^-$. RP-HPLC purity: 95.2% (254 nm) and 96.6% (280 nm); t_r = 12.9 min.

Investigation of Reduction Using RP-HPLC. Each Pt(IV) complex was extracted from its stock solution and added to PBS (200 mM, pH 7.4) except for **2**, which was added to 1:1 v/v of DMSO:PBS (200 mM, pH 7.4) solution (66 μL) in an Eppendorf tube to obtain a concentration of 200 μM. Aqueous sodium ascorbate (NaAsc, 30 equiv) was added to the solutions and mixed at 37 °C in an Eppendorf thermomixer. At regular time intervals, aliquots (30 μL) were taken from the respective reaction mixtures for RP-HPLC analysis. The identities of the products were confirmed by electrospray ionization−mass spectrometry (ESI−MS) analysis and comparison of their retention time with authentic standards.

Fluorescence Measurements. Each compound was extracted from its stock solution and dissolved in PBS (200 mM, pH 7.4) to attain 100 μM. A fixed concentration and volume (100 μM, 200 μL) of each compound was pipetted onto a 96-well black microplate in triplicate. Fluorescence measurements were conducted in which the excitation wavelength was 350 nm, gain setting was 50, and the scanned emission wavelength was from 380 to 700 nm. Complex **2** was dissolved in 1:1 v/v of DMSO:PBS (200 mM, pH 7.4) solution to

https://dx.doi.org/10.1021/acs.inorgchem.0c03299
Inorg. Chem. 2021, 60, 1823−1831

Scheme 1. General Synthetic Strategy of Self-Immolative Pt(IV) Prodrugs

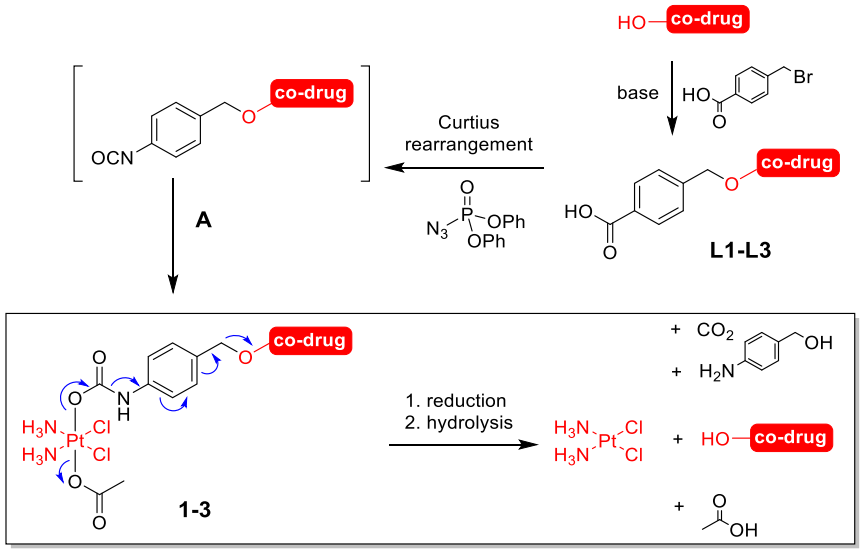

attain 100 μM. NaAsc (30 times concentrated) was added to the solution and mixed on a shaker. A fixed concentration and volume (100 μM, 200 μL) was pipetted onto a 96-well black microplate in triplicate. Fluorescence measurements were conducted in which the excitation wavelength was 350 nm, gain setting was 50, and the scanned emission wavelength was from 380 to 700 nm.

Inhibition of Cell Viability Assay. RP-HPLC studies showed high purity of greater than 95% at both 254 and 280 nm wavelengths for all drugs tested. An MTT stock solution was prepared by dissolving MTT in PBS (5 mg/mL) and storing at 4 °C. Stock solutions of each compound were prepared by dissolving them in DMSO and storing at −20 °C. Concentrations of the Pt(IV) complex stocks were further verified by measuring [Pt] by ICP−OES. HeLa, A2780, and A2780cis cell lines were cultured in complete media (10% FBS in RPMI) at 37 °C under 5% CO_2. Each cell line was seeded at a density of 6000 cells/100 μL per well into 96-well culture plates and incubated for 24 h. Thereafter, the culture media were replaced with fresh complete media (100 μL/well) containing each compound at varying concentrations and maintained for 6 h. The final DMSO concentration in the media was kept below 1% (v/v) to minimize the cytotoxicity of DMSO to the cells. At the end of treatment, the drug-containing media were aspirated and replaced with fresh complete media (100 μL/well) for further 66 h of incubation. The media were then aspirated and replaced with the MTT solution (MTT stock diluted in complete media to 0.5 mg/mL) and incubated for 50 min. The MTT solution was aspirated and replaced with 100 μL/well of DMSO. A BioTek microplate reader was used to determine the UV−vis absorbance at 570 nm. Each drug concentration was measured in sextuplicates, and at least three separate repeats of the experiment were performed. Cytotoxicity was determined with respect to the IC_{50} value determined from dose−response curves (cell viability against log [drug]) plotted from each repeated experiment.

Intracellular Accumulation. Intracellular Pt and In contents were determined using an Agilent 7700 Series ICP−MS (Agilent Technologies, Santa Clara, CA, USA). HeLa cells were seeded into Cellstar 6-well plates (Greiner Bio-One) at a density of 7×10^5 cells per well (2 mL per well). After the cells were allowed to resume exponential growth for 24 h, they were exposed to the compounds of interest at 2.5 μM for 6 h. The cells were trypsinized, neutralized with complete RPMI, and centrifugated at 300 × g for 7 min at 4 °C. Cell pellets were washed twice with 1× PBS and lysed with 100 μL of RIPA lysis buffer for 5 min at 4 °C. The total protein content of each sample was quantified using the bicinchoninic acid (BCA) assay. Equal volume of cell lysates was transferred to 2 mL glass vials and then digested with ultrapure 65% HNO_3 at 110 °C for 72 h. The resulting solution was diluted to 2−4% v/v HNO_3 with ultrapure Milli-Q water and filtered. The Pt content of each sample was quantified by ICP−MS. In was used as an internal standard. Pt and In were measured at m/z = 195 and m/z = 115, respectively. Metal standards for calibration curve (0, 1, 2, 5, 10, 20, 40, and 80 ppb) were freshly prepared before each measurement. All readings were made in triplicate in the He mode.

RESULTS AND DISCUSSION

Design and Synthesis. The design of self-immolative Pt(IV) prodrug complexes involves installing a masked "4-aminobenzyl" linker with the payload attached at the benzyl site and the Pt(IV) motif attached at the amino site via a carbamate group. Upon Pt(IV) reduction, the 4ABA linker would be unmasked, leading to a spontaneous 1,6-elimination reaction to release the codrug (Scheme 1). There are two considerations taken in the design of the synthesis approach. First, amino (or hydroxyl) groups should not be present at *ortho* or *para* positions to the site of conjugation to prevent spontaneous 1,6-elimination. This ruled out the use of simple linker precursors, for example, 4-aminobenzyl bromide, for preparing the ligand intermediate. Second, the weakly nucleophilic hydroxyl ligand on the Pt(IV) scaffold (e.g., **A**) requires a highly electrophilic carboxylating reagent such as acid chloride, anhydride, or isocyanate for reactivity.[35] Our strategy was to use 4-carboxybenzyl bromide to tether the payload and to carry out functional group transformation of the carboxyl moiety into isocyanate followed by acylation with **A** to construct the target Pt(IV) complex. We leveraged on the Curtius rearrangement, which generated an acyl azide intermediate from the carboxyl group that was thermally decomposed into isocyanate with the loss of N_2 gas.[36] Therefore, intermediate ligands **L1−3** and **L3−NO$_2$** were prepared by first reacting the codrug with 4-(bromomethyl)-benzoic acid followed by conversion into isocyanate using DPPA via Curtius rearrangement. Subsequently, the Pt(IV) precursor **A** was reacted with isocyanate in situ to install the masked 4ABA linker on the Pt(IV) scaffold, yielding **1−3** and **3−NO$_2$**. The synthetic strategy of these "release by self-immolation" Pt(IV) prodrugs expanded the existing protocols in the synthesis of multiaction Pt(IV) prodrugs using a traceless linker.

https://dx.doi.org/10.1021/acs.inorgchem.0c03299
Inorg. Chem. 2021, 60, 1823−1831

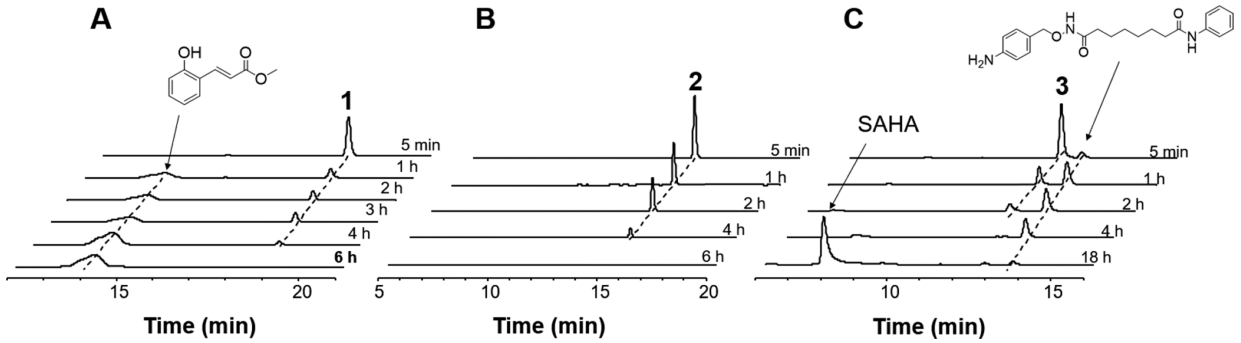

Figure 2. RP-HPLC studies of reduction of self-immolative Pt(IV) prodrugs; **1**–**3** (200 μM) were incubated with 30 equiv NaAsc in PBS (**1** and **3**) or 1:1 v/v DMSO:PBS (**2**) at 37 °C.

Reduction with Concomitant Drug Release by Self-Immolation. To investigate the efficacy of this "release by self-immolation" strategy, the reduction of **1**–**3** was monitored using RP-HPLC and ESI–MS analyses. The complexes were incubated in PBS (20 mM, pH 7.4) at 37 °C, and NaAsc (30 equiv) was used as a model outer-sphere bioreductant. NaAsc has been routinely used for investigating the reduction of both mono- and bis-functionalized Pt(IV) prodrug complexes containing axial carboxylate ligands. Both **1** and **2** exhibited good stability in PBS for more than 24 h (Figure S1) but were completely reduced by NaAsc within 9 h, with **1** being more susceptible to reduction. From the RP-HPLC chromatogram of **1** (Figure 2), we can see that the decrease in the intensity of peak signaling of **1** was accompanied by a simultaneous increase in the peak intensity of MeHC, which was correlated to its expected retention time (t_r). ESI–MS analyses on eluted fractions also confirmed the identity of MeHC (Figure S2). This observation demonstrated that **1** underwent spontaneous 1,6-elimination following Pt(IV) reduction to release MeHC.

For **2**, neither the formation of 7-HMC nor its phenylcarbamate conjugate could be observed on its RP-HPLC chromatogram upon reduction with excess NaAsc (Figure 2). Yet, the treatment of **2** with NaAsc resulted in concomitant restoration of fluorescence emission from 7-HMC, which was indicative of release of the phenylcarbamate linker from the coumarin motif. To investigate this discrepancy, we coincubated 7-HMC with NaAsc and observed their tendency to coelute in the void volume as an ion pair (Figure S3). In the absence of NaAsc, 7-HMC elutes at t_r = 10.4 min. Similar occurrences had been reported for several other substrates in the presence of NaAsc, which would explain the absence of the expected 7-HMC on the RP-HPLC chromatogram.[37] Instead, fluorescence studies were performed to monitor the reduction and elimination kinetics of **2**. When NaAsc was added to **2**, a gradual increase in fluorescence emission at 450 nm was observed as a function of time (Figure 3). This was further confirmed by ESI–MS analysis of the reaction mixture after 6 h, which identified 7-HMC as the product (Figure S4). Fluorescence quenching was observed despite complete reduction, which was attributed to the presence of 4ABA produced.[38,39] These results were in contrast to the α-acetate-tethered 7-HMC Pt(IV) prodrug complex reported by Wang et al. which upon reduction produced a linker artifact tethered to 7-HMC ligands, due to the inability of the ether linkage to dissociate.[17] Therefore, **1** and **2** demonstrated that Pt(IV) prodrug and self-immolation strategies can work efficiently to simultaneously deliver cDDP and an codrug upon intracellular reduction.

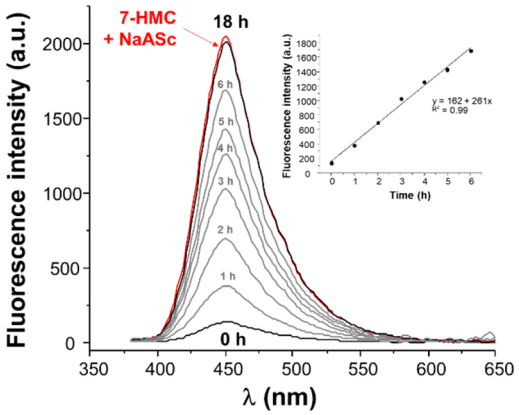

Figure 3. Time course fluorescence emission spectra of **2** after NaAsc treatment; **2** (200 μM) was incubated with 30 equiv NaAsc in 1:1 v/v DMSO:PBS at 37 °C. Equimolar 7-HMC and NaAsc overlaid for comparison (shown in red).

We therefore applied the self-immolation strategy toward the functionalization of SAHA as a codrug. SAHA is a clinically-approved anticancer agent, under the trademark Vorinostat, which acts on chromatin remodeling as a histone deacetylase (HDAC) inhibitor. Crucially, the combination of cDDP and SAHA is synergistic in vitro against a variety of different cell lines in approximately equimolar proportions. Therefore, **3** was prepared using SAHA using the aforementioned strategy by conjugating the linker at the hydroxamic acid functional group on SAHA. The hydroxamic acid moiety is involved in Zn binding and is essential for HDAC inhibition by SAHA. Reduction of **3** by NaAsc was complete within 4 h in keeping with **1** and **2**, but instead of spontaneous elimination, we observed a delayed release of SAHA from the self-immolative linker (Figure 2). A new species at t_r = 13.5 min was identified using ESI–MS to be SAHA tethered to the 4ABA linker (Figure S5). Complete release of SAHA via self-immolation was only accomplished after 18 h, pointing to the lower 1,6-elimination kinetics (Figure 2). We postulated that the slower rate of release was due the stronger hydroxamate ester bonds arising from the α-effect from N-atoms compared to phenolic ethers in **1** and **2**.

To establish whether the self-immolative linker was a viable strategy to enable traceless release of SAHA from a Pt(IV) prodrug scaffold, we considered other alternatives that were reported in the literature. Brabec and co-workers developed a photoactivatable bipyridyl-Pt(IV) azide complex with axial hydroxamate ligands.[40] As far as we know, this is the only

https://dx.doi.org/10.1021/acs.inorgchem.0c03299
Inorg. Chem. 2021, 60, 1823–1831

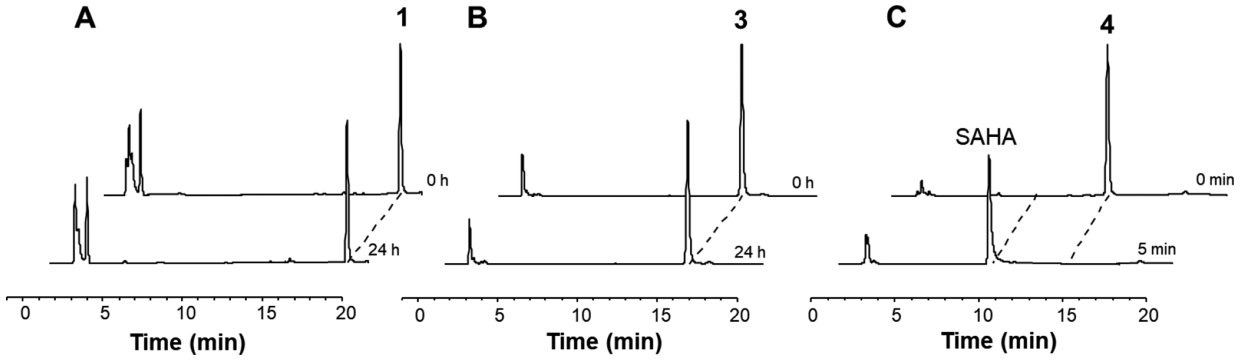

Figure 4. Aqueous stabilities of **1**, **3**, and **4** were analyzed by RP-HPLC; **1**, **3**, and **4** (200 μM) were incubated in PBS at 25 °C.

reported Pt(IV) complex with this unique binding mode but it was unclear whether this design would be compatible with the cDDP scaffold with labile leaving groups. Gibson and co-workers developed a Pt(IV) carbamate complex based on a cDDP scaffold containing a SAHA analogue with a *p*-amino modification on its phenyl ring.[23] This strategy enabled post-functionalization of the Pt(IV) scaffold by installing a labile carbonate axial ligand. The complex efficiently released amino-modified SAHA upon Pt(IV) reduction with decomposition of the carbamate linkage. To avoid modifying SAHA, we adopted Gibson's strategy to directly install SAHA onto the Pt(IV) scaffold via its hydroxamate group using carbonate as a linker. We compared the aqueous stability of the resultant complex **4**, which structurally differed from **3** by the absence of the 4ABA linker. In keeping with the reported Pt(IV) carbonate complexes, **4** exhibited poor aqueous stability in PBS with rapid dissociation of SAHA via hydrolysis as evidenced by RP-HPLC (Figure 4).[41,42] Dissociation can be suppressed using a non-nucleophilic solvent such as DMSO but its instability under aqueous conditions precluded further therapeutic utility. In contrast, **3** exhibited good aqueous stability in PBS and DMSO over extended periods (Figure 4).

The effects of temperature and pH on the reduction rate and self-immolation mechanism were investigated using **3** by RP-HPLC. Increasing pH from 7.4 to 9.0 did not induce rapid and spontaneous release of SAHA (Figure S6); thus, pH conditions did not have a significant influence on the 1,6-elimination of the self-immolative linker within a narrow physiological window. To enhance self-immolation, we stabilized the anionic aniline released during reduction and decarboxylation of the Pt(IV) complex by introducing an electron-withdrawing *meta*-nitro group onto the 4ABA linker unit as **3**−$\mathbf{NO_2}$. The modification did not significantly promote the release of SAHA but retarded it, which suggested that the 1,6-elimination kinetics were governed by the stability of the *p*-aza-quinone-methide species formed rather than the stability of the anionic aniline. This observation was consistent with reports by Rokita, which showed that electron-withdrawing substituents destabilized the *o*-aza-quinone-methide species and could slow down the rate of substrate elimination.[43] Hence, the design strategy for self-immolative Pt(IV) prodrugs must balance both reductive properties of the Pt(IV) prodrug and stability of the resonance structures in the *p*-aza-quinone-methide system. Temperature effects on reduction and elimination kinetics were studied using **3**−$\mathbf{NO_2}$ as the model (Figure S7). We hypothesized that a higher temperature could trigger faster reduction of the Pt(IV) complex and faster 1,6-elimination of the 4ABA unit to release SAHA. Indeed, a higher temperature of 37 °C increased the reduction rates of **3**−$\mathbf{NO_2}$ but had no effect on the 1,6-elimination kinetics of the linker at 25 °C and 37 °C.

Inhibition of Cancer Cell Viability In Vitro. The efficacies of **1** and **2** were measured by evaluating their cell-growth inhibition of HeLa cervical carcinoma cells (Table 1 and Figure S8). At a concentration of up to 200 μM, both MeHC and 7-HMC did not exhibit a significant cytotoxic activity in vitro. This was consistent with previous reports that reported IC_{50} of cinnamate and coumarin derivatives in a mM range.[44,45] Coadministration of cDDP and MeHC or 7-HMC also showed a mediocre activity on HeLa cells. Notably, both **1** and **2** induced significant cytotoxicity against HeLa cancer cells. Complexes **1** and **2** exhibited more than 4- and 1.8-fold increase in cytotoxicity compared to cDDP, respectively, compared to equimolar mixtures of cDDP and the codrug. The conjugation of hydrophobic bulky carbamate ligands to cDDP gave rise to Pt(IV) complexes **1** and **2** endowed with higher lipophilicities and greater propensities to be taken up intracellularly compared to cDDP.[46−48] Therefore, the increased activity in **1** and **2** was most likely attributed to the higher lipophilicity of **1** and **2** that resulted in greater cellular uptake as well as improved delivery of the codrug payload. This was further supported by cellular uptake studies of cDDP, **1**, and **2** in the HeLa cell line (Table 1 and Figure S9) at equimolar Pt concentrations (2.5 μM for 6 h), which

Table 1. Inhibition of Cell Viability in the HeLa Cell Line and Cellular Accumulation

entry	IC_{50} [μM][a]	intracellular Pt content (nmol Pt/mg protein)[b]
cDDP	10.0 ± 0.5	0.05 ± 0.01
MeHC	>100	
7-HMC	>100	
4ABA	>2000	
cDDP + MeHC (1:1)	10.2 ± 0.3	
cDDP + 7-HMC (1:1)	10.5 ± 1.6	
1	2.4 ± 0.1	0.62 ± 0.10
2	5.5 ± 1.0	1.78 ± 1.10

[a]IC_{50} value is the concentration of the compound needed to inhibit cell growth by 50% and is determined using the MTT assay and corrected with actual [Pt] determined by ICP−OES. Data presented are the calculated averages of at least three separate studies and their standard deviations. [b]Pt content was determined by ICP−MS and protein content using the BCA assay.

https://dx.doi.org/10.1021/acs.inorgchem.0c03299
Inorg. Chem. 2021, 60, 1823−1831

showed significantly higher Pt accumulation for **1** and **2** compared to cDDP.

Several reports had pointed toward the coadministration of SAHA and cDDP as being synergistic in inducing cancer cell death.[29−31] In particular, the concurrent use of SAHA and cDDP resulted in favorable dose reductions against several Pt-resistant ovarian carcinoma cell lines, indicating their potential as a combination therapy for recurrent ovarian tumors.[29] Hence, the antiproliferative efficacies of **3** and **3−NO$_2$** were measured by evaluating their cell-growth inhibition of Pt-sensitive A2780 and Pt-resistant A2780cis ovarian carcinoma cells (Table 2 and Figure S10). None of the Pt(IV)−SAHA prodrugs were more cytotoxic than cDDP and coadministration of cDDP and SAHA against A2780 cells. However, the self-immolative Pt(IV) prodrugs were equally cytotoxic to cDDP-resistant A2780cis cells with a resistance factor of 1.2, which was significantly lower than cDDP's resistance factor of 14.0. Complex **4** also exhibited high cytotoxicity against A2780 and A2780cis cells at concentrations approximate to the cDDP + SAHA mixture, presumably due to premature release of SAHA by rapid hydrolysis of **4**.

Table 2. Inhibition of Cell Viability in Pt-Sensitive A2780 and Pt-Resistant A2780cis Cell Lines

entry	IC_{50} [μM][a]		
	A2780	A2780cis	resistance factor[b]
cDDP	1.1 ± 0.3	15.8 ± 2.9	14.0
SAHA	14.7 ± 3.7	13.9 ± 3.5	0.9
cDDP + SAHA (1:1)	1.1 ± 0.2	5.5 ± 0.3	5.1
4ABA	>2000	>2000	n.d.
3	4.2 ± 0.2	5.2 ± 1.5	1.2
3−NO$_2$	7.2 ± 1.8	7.6 ± 1.1	1.2
4	2.3 ± 0.6	4.7 ± 0.9	2.0

[a]IC_{50} value is the concentration of the compound needed to inhibit cell growth by 50% and is determined using the MTT assay and corrected with actual [Pt] determined by ICP−OES. Data presented are the calculated averages of at least three separate studies and their standard deviations. [b]Resistance factor is the ratio between the IC_{50} values of A2780cis to A2780.

CONCLUSIONS

By combining the Pt(IV) prodrug scaffold with self-immolative linkers, we developed a new class of Pt(IV) prodrug complexes that are rationally designed for traceless and synchronous delivery of cDDP and a codrug. The complexes were constructed sequentially from the ligand end and a crucial functional group transformation was carried out to install the desired carbamate conjugate on the Pt(IV) scaffold while avoiding premature self-immolation. These novel complexes were activated upon reduction at the Pt(IV) center, which cleaved the functionalized carbamate ligand to yield cDDP. Decomposition of the carbamate ligand initiated the self-immolation of the masked 4ABA linker to release the codrug. Investigation of the reduction and release mechanism showed the viability of this approach, particularly for codrugs containing phenolic functional groups. This strategy can overcome the challenge in the development of multiaction Pt(IV) prodrug complexes that typically employed ether, amide, or ester linkers for conjugation, which would leave a linker artifact on the codrug. For other complex functional groups such as hydroxamate in SAHA, the approach was limited by the slower 1,6-elimination kinetics of the linker. This strategy paves the way for a traceless codelivery system of cDDP and an organic codrug for ratiometric and synchronous activation within an intracellular environment.

ASSOCIATED CONTENT

Supporting Information

The Supporting Information is available free of charge at https://pubs.acs.org/doi/10.1021/acs.inorgchem.0c03299.

HPLC chromatograms of **1−4** and **3−NO$_2$** under different reaction conditions; dose−response curves of tested compounds in vitro; and spectroscopic data for synthesized compounds, namely, MeHC, SAHA, **L1−L3**, **L3−NO$_2$**, **1−4**, and **3−NO$_2$** (PDF)

AUTHOR INFORMATION

Corresponding Author

Wee Han Ang − *Department of Chemistry, National University of Singapore, Singapore 117543, Singapore; NUS Graduate School of Integrative Sciences and Engineering, National University of Singapore, Singapore 119077, Singapore;* orcid.org/0000-0003-2027-356X; Email: ang.weehan@nus.edu.sg

Authors

Violet Eng Yee Lee − *Department of Chemistry, National University of Singapore, Singapore 117543, Singapore; NUS Graduate School of Integrative Sciences and Engineering, National University of Singapore, Singapore 119077, Singapore*

Zhi Chiaw Lim − *Department of Chemistry, National University of Singapore, Singapore 117543, Singapore*

Suet Li Chew − *Department of Chemistry, National University of Singapore, Singapore 117543, Singapore*

Complete contact information is available at: https://pubs.acs.org/10.1021/acs.inorgchem.0c03299

Author Contributions

The manuscript was written through contributions of V.E.Y.L. and W.H.A. All authors have given approval to the final version of the manuscript.

Notes

The authors declare no competing financial interest.

ACKNOWLEDGMENTS

We acknowledge financial support from the Ministry of Education and National University of Singapore (R143-000-A66-114). V.E.Y.L. acknowledges the scholarship and support from the NUS Graduate School for Integrative Sciences and Engineering (NGS). The content of this paper has been partly published in V.E.Y.L.'s doctoral dissertation.

REFERENCES

(1) Johnstone, T. C.; Suntharalingam, K.; Lippard, S. J. The next generation of platinum drugs: targeted Pt(II) agents, nanoparticle delivery, and Pt(IV) prodrugs. *Chem. Rev.* **2016**, *116*, 3436−3486.

(2) Galluzzi, L.; Senovilla, L.; Vitale, I.; Michels, J.; Martins, I.; Kepp, O.; Castedo, M.; Kroemer, G. Molecular mechanisms of cisplatin resistance. *Oncogene* **2012**, *31*, 1869−1883.

(3) Chou, T.-C. Theoretical Basis, experimental design, and computerized simulation of synergism and antagonism in drug combination studies. *Pharmacol. Rev.* **2006**, *58*, 621−681.

(4) Wang, H.; Huang, Y. Combination therapy based on nano codelivery for overcoming cancer drug resistance. *Med. Drug Discov.* **2020**, *6*, No. 100024.
(5) Miao, L.; Guo, S.; Zhang, J.; Kim, W. Y.; Huang, L. Nanoparticles with precise ratiometric co-loading and co-delivery of gemcitabine monophosphate and cisplatin for treatment of bladder cancer. *Adv. Funct. Mater.* **2014**, *24*, 6601−6611.
(6) Leary, M.; Heerboth, S.; Lapinska, K.; Sarkar, S. Sensitization of drug resistant cancer cells: A Matter of combination therapy. *Cancers* **2018**, *10*, 483.
(7) Hambley, T. W. Transporter and protease mediated delivery of platinum complexes for precision oncology. *J. Biol. Inorg. Chem.* **2019**, *24*, 457−466.
(8) Chin, C. F.; Wong, D. Y. Q.; Jothibasu, R.; Ang, W. H. Anticancer Platinum (IV) Prodrugs with Novel Modes of Activity. *Curr. Top. Med. Chem.* **2011**, *11*, 2602−2612.
(9) Rosell, R.; Gatzemeier, U.; Betticher, D. C.; Keppler, U.; Macha, H. N.; Pirker, R.; Berthet, P.; Breau, J. L.; Lianes, P.; Nicholson, M.; Ardizzoni, A.; Chemaissani, A.; Bogaerts, J.; Gallant, G. Phase III randomised trial comparing paclitaxel/carboplatin with paclitaxel/cisplatin in patients with advanced non-small-cell lung cancer: A cooperative multinational trial. *Ann. Oncol.* **2002**, *13*, 1539−1549.
(10) Lopes, F.; Liu, J.; Morgan, S.; Matthews, R.; Nevin, L.; Anderson, R. A.; Spears, N. Single and combined effects of cisplatin and doxorubicin on the human and mouse ovary in vitro. *Reproduction* **2020**, *159*, 193.
(11) Chin, C. F.; Yap, S. Q.; Li, J.; Pastorin, G.; Ang, W. H. Ratiometric delivery of cisplatin and doxorubicin using tumour-targeting carbon-nanotubes entrapping platinum(IV) prodrugs. *Chem. Sci.* **2014**, *5*, 2265−2270.
(12) Lee, Y. J.; Doliny, P.; Gomez-Fernandez, C.; Powell, J.; Reis, I.; Hurley, J. Docetaxel and cisplatin as primary chemotherapy for treatment of locally advanced breast cancers. *Clin. Breast Cancer* **2004**, *5*, 371−376.
(13) Malik, I. A.; Aziz, Z.; Zaidi, M. S. H.; Sethuraman, G. Gemcitabine and cisplatin is a highly effective combination chemotherapy in patients with advanced cancer of the gallbladder. *Am. J. Clin. Oncol.* **2003**, *26*, 174−177.
(14) Jin, S.; Guo, Y.; Song, D.; Zhu, Z.; Zhang, Z.; Sun, Y.; Yang, T.; Guo, Z.; Wang, X. Targeting Energy metabolism by a platinum(IV) Prodrug as an alternative pathway for cancer suppression. *Inorg. Chem.* **2019**, *58*, 6507−6516.
(15) Guo, Y.; Zhang, S.; Yuan, H.; Song, D.; Jin, S.; Guo, Z.; Wang, X. A platinum(IV) prodrug to defeat breast cancer through disrupting vasculature and inhibiting metastasis. *Dalton Trans.* **2019**, *48*, 3571−3575.
(16) Ma, L.; Ma, R.; Wang, Y.; Zhu, X.; Zhang, J.; Chan, H. C.; Chen, X.; Zhang, W.; Chiu, S.-K.; Zhu, G. Chalcoplatin, a dual-targeting and p53 activator-containing anticancer platinum(IV) prodrug with unique mode of action. *Chem. Commun.* **2015**, *51*, 6301−6304.
(17) Wang, Q.; Chen, Y.; Li, G.; Liu, Z.; Ma, J.; Liu, M.; Li, D.; Han, J.; Wang, B. Synthesis and evaluation of bi-functional 7-hydroxycoumarin platinum(IV) complexes as antitumor agents. *Biorg. Med. Chem.* **2019**, *27*, 2112−2121.
(18) Huang, X.; Huang, R.; Gou, S.; Wang, Z.; Liao, Z.; Wang, H. Combretastatin A-4 Analogue: A dual-targeting and tubulin inhibitor containing antitumor Pt(IV) moiety with a unique mode of action. *Bioconjugate Chem.* **2016**, *27*, 2132−2148.
(19) Barnes, K. R.; Kutikov, A.; Lippard, S. J. Synthesis, characterization, and cytotoxicity of a series of estrogen-tethered platinum(IV) complexes. *Chem. Biol.* **2004**, *11*, 557−564.
(20) Wong, D. Y. Q.; Lau, J. Y.; Ang, W. H. Harnessing chemoselective imine ligation for tethering bioactive molecules to platinum(IV) prodrugs. *Dalton Trans.* **2012**, *41*, 6104−6111.
(21) Wong, D. Y. Q.; Yeo, C. H. F.; Ang, W. H. Immunochemotherapeutic platinum(IV) prodrugs of cisplatin as multimodal anticancer agents. *Angew. Chem., Int. Ed.* **2014**, *53*, 6752−6756.
(22) Yempala, T.; Babu, T.; Karmakar, S.; Nemirovski, A.; Ishan, M.; Gandin, V.; Gibson, D. Expanding the arsenal of Pt^{IV} anticancer agents: Multi-action Pt^{IV} anticancer agents with bioactive ligands possessing a hydroxy functional group. *Angew. Chem., Int. Ed.* **2019**, *58*, 18218−18223.
(23) Babu, T.; Sarkar, A.; Karmakar, S.; Schmidt, C.; Gibson, D. Multiaction Pt(IV) carbamate complexes can codeliver Pt(II) Drugs and amine containing bioactive molecules. *Inorg. Chem.* **2020**, *59*, 5182−5193.
(24) Chen, S.; Yao, H.; Zhou, Q.; Tse, M.-K.; Gunawan, Y. F.; Zhu, G. Stability, reduction, and cytotoxicity of platinum(IV) anticancer prodrugs bearing carbamate axial ligands: comparison with their carboxylate analogues. *Inorg. Chem.* **2020**, *59*, 11676−11687.
(25) Blencowe, C. A.; Russell, A. T.; Greco, F.; Hayes, W.; Thornthwaite, D. W. Self-immolative linkers in polymeric delivery systems. *Polym. Chem.* **2011**, *2*, 773−790.
(26) Gan, F. F.; Scarmagnani, Y. S. C. S.; Palaniappan, P.; Franks, M.; Poobalasingam, T. D.; Bradshaw, T.; Westwell, A. D.; Hagen, T. Structure−activity analysis of 2′-modified cinnamaldehyde analogues as potential anticancer agents. *Biochem. Biophys. Res. Commun.* **2009**, *387*, 741−747.
(27) Walkinshaw, D. R.; Yang, X. J. Histone deacetylase inhibitors as novel anticancer therapeutics. *Curr. Oncol.* **2015**, *10*, 145−162.
(28) Idippily, N. D.; Gan, C.; Orefice, P.; Peterson, J.; Su, B. Synthesis of Vorinostat and cholesterol conjugate to enhance the cancer cell uptake selectivity. *Bioorg. Med. Chem. Lett.* **2017**, *27*, 816−820.
(29) Ong, P.-S.; Wang, X.-Q.; Lin, H.-S.; Chan, S. Y.; Ho, P. S. Synergistic effects of suberoylanilide hydroxamic acid combined with cisplatin causing cell cycle arrest independent apoptosis in platinum-resistant ovarian cancer cells. *Int. J. Oncol.* **2012**, *40*, 1705−1713.
(30) Hou, M.; Huang, Z.; Chen, S.; Wang, H.; Feng, T.; Yan, S.; Su, Y.; Zuo, G. Synergistic antitumor effect of suberoylanilide hydroxamic acid and cisplatin in osteosarcoma cells. *Oncol. Lett.* **2018**, *16*, 4663−4670.
(31) Asgar, M. A.; Senawong, G.; Sripa, B.; Senawong, T. Synergistic anticancer effects of cisplatin and histone deacetylase inhibitors (SAHA and TSA) on cholangiocarcinoma cell lines. *Int. J. Oncol.* **2016**, *48*, 409−420.
(32) Dhara, S. A rapid method for the synthesis of *cis*-$[Pt(NH_3)_2Cl_2]$. *Indian J. Chem.* **1970**, *8*, 193−194.
(33) Yao, H.; Xu, Z.; Li, C.; Tse, M.-K.; Tong, Z.; Zhu, G. Synthesis and cytotoxic study of a platinum(IV) anticancer prodrug with selectivity toward luteinizing hormone-releasing hormone (LHRH) receptor-positive cancer cells. *Inorg. Chem.* **2019**, *58*, 11076−11084.
(34) Chung, Y.-M.; El-Shazly, M.; Chuang, D.-W.; Hwang, T.-L.; Asai, T.; Oshima, Y.; Ashour, M. L.; Wu, Y.-C.; Chang, F.-R. Suberoylanilide Hydroxamic acid, a histone deacetylase inhibitor, induces the production of anti-inflammatory cyclodepsipeptides from beauveria felina. *J. Nat. Prod.* **2013**, *76*, 1260−1266.
(35) Wilson, J. J.; Lippard, S. J. Synthesis, characterization, and cytotoxicity of platinum(IV) carbamate complexes. *Inorg. Chem.* **2011**, *50*, 3103−3115.
(36) Curtius, T. 20. Hydrazide und azide organischer säuren i. abhandlung. *J. Prakt. Chem.* **1894**, *50*, 275−294.
(37) Sattar, A.; Willman, J. E.; Kolluri, R. Possible warfarin resistance due to interaction with ascorbic acid: Case report and literature review. *Am. J. Health-Syst. Pharm.* **2013**, *70*, 782−786.
(38) Bhavya, P.; Melavanki, R.; Kusanur, R.; Sharma, K.; Muttannavar, V. T.; Naik, L. R. Effect of viscosity and dielectric constant variation on fractional fluorescence quenching analysis of coumarin dye in binary solvent mixtures. *Luminescence* **2018**, *33*, 933−940.
(39) Evale, B. G.; Hanagodimath, S. M. Static and dynamic quenching of biologically active coumarin derivative by aniline in benzene−acetonitrile mixtures. *J. Lumin.* **2010**, *130*, 1330−1337.
(40) Kasparkova, J.; Kostrhunova, H.; Novakova, O.; Křikavová, R.; Vančo, J.; Trávníček, Z.; Brabec, V. A photoactivatable platinum(IV)

https://dx.doi.org/10.1021/acs.inorgchem.0c03299
Inorg. Chem. 2021, 60, 1823−1831

complex targeting genomic dna and histone deacetylases. *Angew. Chem., Int. Ed.* **2015**, *54*, 14478−14482.
(41) Wexselblatt, E.; Yavin, E.; Gibson, D. Platinum(IV) prodrugs with haloacetato ligands in the axial positions can undergo hydrolysis under biologically relevant conditions. *Angew. Chem., Int. Ed.* **2013**, *52*, 6059−6062.
(42) Dhar, S.; Lippard, S. J. Mitaplatin, a potent fusion of cisplatin and the orphan drug dichloroacetate. *Proc. Natl. Acad. Sci. U. S. A.* **2009**, *106*, 22199−22204.
(43) Weinert, E. E.; Dondi, R.; Colloredo-Melz, S.; Frankenfield, K. N.; Mitchell, C. H.; Freccero, M.; Rokita, S. E. Substituents on quinone methides strongly modulate formation and stability of their nucleophilic adducts. *J. Am. Chem. Soc.* **2006**, *128*, 11940−11947.
(44) Li, F.; Awale, S.; Tezuka, Y.; Kadota, S. Cytotoxicity of constituents from mexican propolis against a panel of six different cancer cell lines. *Nat. Prod. Commun.* **2010**, *5*, 1601−1606. 1934578X1000501018
(45) Faridoon; Edkins, A. L.; Isaacs, M.; Mnkandhla, D.; Hoppe, H. C.; Kaye, P. T. Synthesis and evaluation of substituted 4-(N-benzylamino)cinnamate esters as potential anti-cancer agents and HIV-1 integrase inhibitors. *Bioorg. Med. Chem. Lett.* **2016**, *26*, 3810−3812.
(46) Raveendran, R.; Braude, J. P.; Wexselblatt, E.; Novohradsky, V.; Stuchlikova, O.; Brabec, V.; Gandin, V.; Gibson, D. Pt(IV) derivatives of cisplatin and oxaliplatin with phenylbutyrate axial ligands are potent cytotoxic agents that act by several mechanisms of action. *Chem. Sci.* **2016**, *7*, 2381−2391.
(47) Gibson, D. Platinum(IV) anticancer prodrugs - hypotheses and facts. *Dalton Trans.* **2016**, *45*, 12983−12991.
(48) Ravera, M.; Gabano, E.; McGlinchey, M. J.; Osella, D. A view on multi-action Pt(IV) antitumor prodrugs. *Inorg. Chim. Acta* **2019**, *492*, 32−47.

https://dx.doi.org/10.1021/acs.inorgchem.0c03299
Inorg. Chem. 2021, 60, 1823−1831